Journal of Photochemistry and Photobiology A: Chemistry 210 (2010) 193–199

Contents lists available at ScienceDirect

Journal of Photochemistry and Photobiology A: Chemistry

journal homepage: www.elsevier.com/locate/jphotochem

Physico-chemical properties and photo-reactivity relationship for *para*-substituted phenols in photo-assisted Fenton system

F. Mazille[a], T. Schoettl[a], A. Lopez[b], C. Pulgarin[a,*]

[a] Institute of Chemical Sciences and Engineering, SB, GGEC, Ecole Polytechnique Fédérale de Lausanne, 1015 Lausanne, Switzerland
[b] Istituto di Ricerca Sulle Acque C.N.R, Via F. De Blasio 5, 70123 Bari, Italy

ARTICLE INFO

Article history:
Received 5 November 2009
Received in revised form 8 December 2009
Accepted 15 December 2009
Available online 23 December 2009

Keywords:
Physico-chemical descriptors
Photo-Fenton
Structure–reactivity relationship
Water detoxification

ABSTRACT

The reactivity of phenolic compounds can be drastically affected by the electronic nature of the substituting groups. In this work, the effect of physico-chemical properties on the reactivity via photo-assisted Fenton catalysis is reported for several *para*-substituted phenols (*p*-nitrophenol (*p*-NO_2), *p*-chlorophenol (*p*-Cl), *p*-hydroxybenzaldehyde (*p*-CHO), phenol (p-H), *p*-methoxyphenol (*p*-OCH_3), *p*-hydroxyphenol (p-OH)) in order to cover a wide range of electronics effects. Electronic descriptors (Hammett constants (σ), frontier molecular orbital energies (E_{HOMO}), electronic and zero point energies (E, E_{ZERO})), electrochemical descriptor (half wave potential for the oxidation of phenols to phenoxyl radical ($E_{1/2}$)), and other descriptors (acidity constants (pK_a), maximum absorption wavelength (λ_{max}), 1-octanol/water partition coefficient (K_{ow})) were correlated with the initial Fenton and photo-Fenton degradation rates (r_0). Linear relationships were obtained between the initial Fenton and photo-Fenton degradation rates and electronic descriptors. However *p*-Cl and *p*-CHO showed higher photo-Fenton degradation rates than ones predicted by the model implying the presence of weaker bonds in these molecules. The biodegradability increase due to the photo-Fenton process was strong but poorly selective suggesting that the produced intermediates present a similar biodegradability.

1. Introduction

The Fenton reaction is an advanced oxidation process that underlines generation of highly reactive hydroxyl radicals (•OH) from a mixture of ferrous ions (Fe^{2+}) and hydrogen peroxide (H_2O_2) according to the Haber–Weiss cycle Eqs. (1)–(4). This reaction is currently of interest in the remediation of water that has been contaminated by toxic and recalcitrant organic pollutants because the added iron ions and H_2O_2 are easy to handle and environmentally benign:

$$Fe(II) + H_2O_2 \rightarrow Fe(III) + OH^- + OH^\bullet (k = 40\text{–}80\ M/s) \quad (1)$$

$$Fe(III) + H_2O_2 \rightarrow Fe(II) + HO_2{}^{-\bullet} + H^+ (k = 0.003\ M/s) \quad (2)$$

$$Fe(III) + HO_2{}^{-\bullet}/O_2{}^{-\bullet} \rightarrow Fe(II) + O_2 \quad (3)$$

$$Fe(III) + HO_2{}^{-\bullet}/O_2{}^{-\bullet} \rightarrow Fe(III) + H_2O_2 \quad (4)$$

The rate-limiting step of the overall reaction is the reduction of Fe(III) to Fe(II). Fenton rates are increased by light irradiation in the presence of ligands leading to photo-Fenton reaction (Eqs. (5) and (6)). The presence of both Fe-absorbing complexes an light accelerates the regeneration of Fe(II) ions by a ligand to metal charge transfer (LMCT) leading to additional hydroxyl radical formation. OH• radicals can also be formed by H_2O_2 photolysis (Eq. (7)). However, although the quantum yield of H_2O_2 photolysis is high, photolysis scarcely takes place due to (i) the low molecular absoptivity of H_2O_2 at wavelength >320 nm and (ii) the low proportion photons with wavelength <320 nm in the solar radiation:

$$Fe(III)(OH)^{2+} + h\nu \rightarrow Fe(II) + OH^\bullet \quad (5)$$

$$Fe(III)L_n + h\nu \rightarrow Fe(II)L_{n-1} + L_{OH}{}^{+\bullet} \quad (6)$$

$$H_2O_2 + h\nu \rightarrow 2OH^\bullet \quad (7)$$

The photocatalytic degradation rate of different compounds depends on various parameters, such as temperature, pH, initial concentration of the pollutant, Fe^{2+} an H_2O_2 concentrations, light intensity, and chemical nature (structure) of the reactants. The photochemical degradation of phenol and its derivates using TiO_2 photocatalysis [1–8] or photo-Fenton oxidation [9–14] has been reported during the last decade. The catalytic degradation is affected by the number of substitutents, their electronic nature and their position in the aromatic ring [15–24]. In particular Parra et al. [20] and Torres et al. [21] have reported quantitative structure–reactivity relationships (QSRR) during the degradation

* Corresponding author at: Swiss Federal Institute of Technology, Group of Electrochemical Engineering, Lausanne, Switzerland. Tel.: +41 21 693 47 20; fax: +41 21 693 6161.
E-mail address: cesar.pulgarin@epfl.ch (C. Pulgarin).

1010-6030/$ – see front matter © 2009 Elsevier B.V. All rights reserved.
doi:10.1016/j.jphotochem.2009.12.015

of *para*-substituted phenols for TiO_2 photocatalysis and electrocatalytic oxidation, respectively. Their results have shown correlation between molecular structure and the kinetic parameters showing that *p*-halogen-phenols react in a different way than their non-halogenated analogues. A recent study predicted the oxidation positions in the benzene ring using frontier electron density theory to describe the reactivity [25]. In photo-Fenton processes, only few reports are available on nitrophenol degradation [26,27], cyclic organic water contaminant [28] and for polychlorinated dibenzo-*p*-dioxins [29]. However no systematic correlation of molecular structure and degradation kinetics was performed.

In this work, the Hammett constants (σ), 1-octanol/water partition coefficient (K_{ow}), calculated energy of the highest occupied molecular orbital (E_{HOMO}), zero point energy (E_{ZERO}) and experimental half-wave potential ($E_{1/2}$) were correlated with the experimental initial rates of degradation calculated with Eq. (8):

$$r_0 = \frac{[\text{Substance}]_0 - [\text{Substance}]_t}{t} \quad (8)$$

Hammett constants (σ) describe the effect different substituent induced on the electronic density of the aromatic ring. σ directly relates the ionization potential and the susceptibility of a molecule to undergo electrophilic attack. The energy of the highest occupied molecular orbital (E_{HOMO}) is a useful parameter to model radical reactions and was calculated by Aptula et al. [30]. K_{ow} represents the molecular hydrophobicity of a given compound. A high value of K_{ow} (>1000) means that the molecule has a great affinity for organic solvents but not for water. Some studies have correlated K_{ow} with the molecular biological properties. The half wave potential ($E_{1/2}$) corresponds to the oxidation of phenols to phenoxyl radicals via Eq. (9). The zero point energies where calculated by Gross et al. [32]. The absorption peaks were measured by UV–vis spectrophotometry:

$$PhOH \rightarrow PhO^{\bullet} + H^{+} + e^{-} \quad (9)$$

The biodegradability of substituted phenols solutions depends on electronic effects, on their transport ability through the bacteria membranes and on the toxic effect of a given substituent. In this study, the biodegradability of *para*-substituted phenol solutions degraded by a photo-Fenton process was determined to see how the nature of the substituent affects the biodegradability of the generated degradation intermediate.

2. Experimental

2.1. Chemicals

The used organic compounds: phenol (p-H), 4-nitrophenol (*p*-NO_2), 4-chlorophenol (*p*-Cl), 4-hydroxybenzaldehyde (*p*-CHO), 4-hydroxyphenol (p-OH) and iron sulfate (II) heptahydrated, were supplied by Flucka, 4-methoxyphenol (*p*-OCH_3) by Acros Organics. Ferrous iron sulfate ($FeSO_4{\cdot}7H_2O$) as well as the solutions of sodium bisulfite (38–40%) and hydrogen peroxide (35%) stabilized, were supplied by Sigma–Aldrich, the nitric acid (65%) by VWR BDA Prolabo.

2.2. Photoreactor and irradiation procedures

All degradation experiments were carried out under simulated solar light, using thin film Pyrex glass reactors with an illuminated volume of 25 mL (Fig. 1). A peristaltic pump allows circulation of the water from a glass bottle acting as recirculation tank, to the reactors with a flow rate of 100 mL/min. The total volume of the system (110 mL) can be distinguished in two parts: 25 mL irradiated volume and the dead volume. The reactor was illuminated in the cavity of a solar simulator CPS Suntest system (Atlas GmbH).

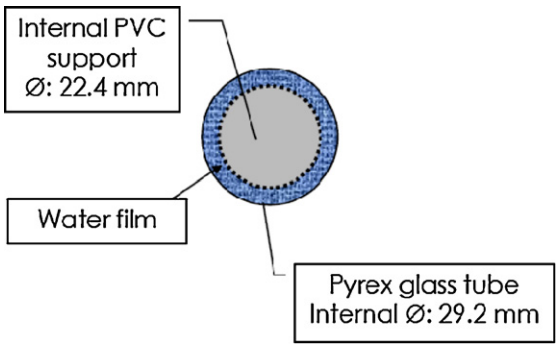

Fig. 1. Transversal cut and characteristics of the photo-reactor.

This solar box has a spectral distribution of about 0.5% of the emitted photons at wavelengths shorter than 300 nm, and about 7% within 300 and 400 nm. The emission spectrum between 400 and 800 nm follows the solar spectrum. The temperature of the solution increased up to approximately 30 °C during the course of the reaction. Control experiments in the dark were performed under similar conditions. Three reactors have been placed in parallel inside the solar box (Fig. 2). The degradation experiments were performed using para-substituted phenols solutions (1.8 mM), each compound in separated solutions. All the experiments were performed in triplicate and the presented results corresponds to the average.

2.3. Analysis of the irradiated solutions

The quantitative determination of organic compounds was carried out by HPLC chromatography using a LC system HPLC-UV: Shimatzu LC-2010A equipped with a UV detector. Samples, injected via autosampler, were eluted at a flow rate of 1 mL/min through a column (Nucleosil C18, Marcherey-Nagel) using as mobile phase acetonitrile–acetic acid solution (10%) in a 40/60 ratio. The total organic carbon (TOC) was monitored via a (Shimadzu 500) instrument equipped with an ASI automatic sample injector. The peroxide concentrations were determined by Merkoquant® paper at levels between 0.5 and 25 mg/L. The UV–vis spectrums were recorded using a Varian Cary 1E UV–vis spectrophotometer. The BOD_5 was determined measuring the oxygen consumption during the biochemical degradation of the organic compounds. This analysis was made by means of a WTW 2000 Oxitop unit thermostated at 20 °C. The pH was adjusted between 6.8 and 7.5 and 1 mL of decanted sludge (inoculums from the biological plant of Morges, Switzerland) was added to the solutions.

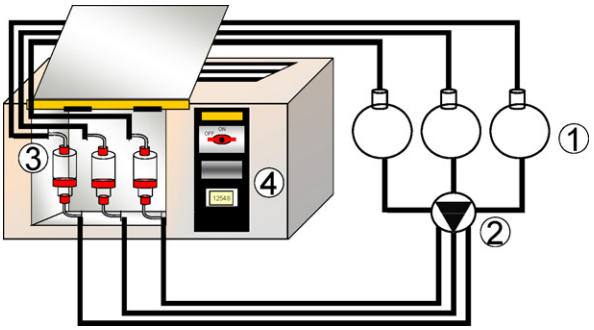

Fig. 2. Photocatalytic setup: (1) tanks, (2) peristatic pump, (3) photoreactors, and (4) solar simulator.

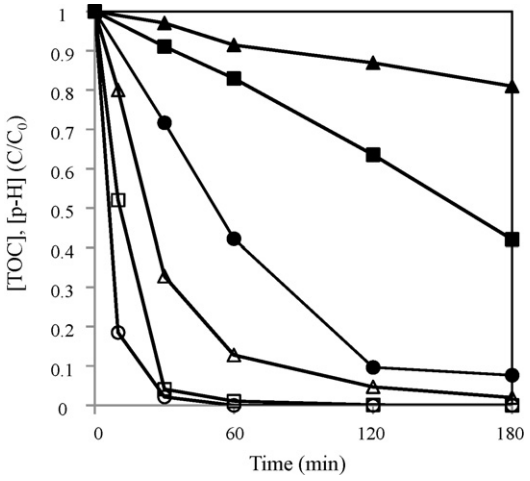

Fig. 3. Substance (unfilled symbols) and TOC (filled symbols) removal during photo-Fenton degradation of phenol (1.8 mM) for different Fe^{2+} concentrations (-●-: 1 mg/L; -■-: 3 mg/L; -▲-: 10 mg/L) in the presence of H_2O_2 (15 mM).

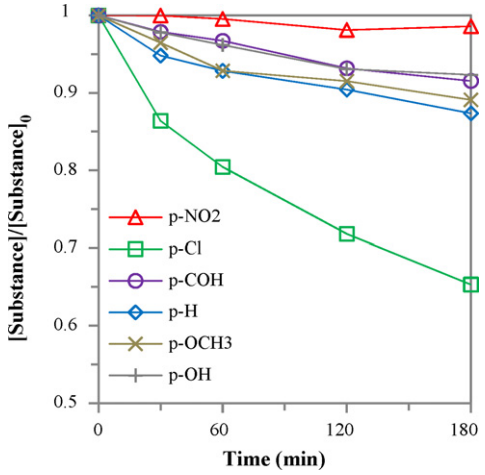

Fig. 4. Evolution of *para*-substituted phenols concentration during photolysis in the presence of Fe^{2+} (3 mg/L) at pH = 3.

3. Results and discussion

3.1. Preliminary experiments

3.1.1. Selection of Fenton reactant concentration

The concentration of the Fenton reagents (Fe^{2+}/H_2O_2) during pollutant degradation has to be chosen carefully, to be able to observe the slight differences caused by the different substituents. In the case of photo-Fenton degradation of 2 mM phenol, Kavitha et al. [13] have reported that optimal concentrations are [Fe^{2+}] = 45 mg/L and [H_2O_2] = 30 mM.

Fig. 3 presents the evolution of phenol and TOC concentrations during photo-Fenton oxidation for different Fe^{2+} concentrations (1, 3 and 10 mg/L) in the presence of H_2O_2 (15 mM). Fig. 3 shows that total phenol degradation is achieved in 3 h and that the initial degradation rate depends on iron concentration leading to 10, 50 and 80% abatement within 15 min for 1, 3 and 10 mg/L, respectively. Fig. 3 shows as well that the mineralization process is dependent on [Fe^{2+}], with 20, 60, 95% TOC removal for [Fe^{2+}] = 1, 3 and 10 mg/L, respectively. For the intermediate concentration of 3 mg/L, the degradation is not too fast and TOC removal is sufficient to allow the reaction to be compared with other substituted phenols. This concentration was chosen to assess the effect of the substituent group nature on the Fenton and photo-Fenton degradation rates.

3.1.2. UV–vis spectrum measurements

The UV–vis spectrum (between 200 and 800 nm) of solution of *para*-substituted phenols (0.05 mM) at pH = 3 in the presence and in the absence of 0.18 mM $FeSO_4$ was measured (results not shown here). It was observed that all the *para*-substituted phenols absorb between 250 and 350 nm (Table 1). In the presence of Fe^{2+} in *para*-substituted phenols solutions, the iron complex formation proceeded only with p-OH and *p*-OCH_3.

3.1.3. Photolysis experiments

Under irradiation at pH 3, no significant degradation (<5%) of *para*-substituted phenols was observed (results not shown here). The addition of Fe^{2+} considerably affected the compounds reactivity. For *p*-OCH_3, p-OH, p-H and p-COH a degradation of about 10% was attained within 3 h (see Fig. 4). Although p-OH and *p*-OCH_3 form complexes with Fe^{2+}, these compounds showed similar degradation rates that the other para-substituted phenols, in the presence of Fe^{2+} and light. *p*-NO_2 degradation remained unchanged when Fe^{2+} was present or not. In the case of *p*-Cl, the presence of Fe^{2+} accelerated the degradation leading to 35% *p*-Cl degradation after 3 h irradiation. In order to determine if the *p*-Cl photodegradation in the presence of Fe^{2+} was due to the effect of light, we run the degradation of *p*-Cl solution in the dark. Fig. 5 shows that the presence of Fe^{2+} ions in the dark (trace a) was sufficient to degrade 20% of *p*-Cl within 3 h. Light irradiation was seen to accelerate the degradation (trace b).

3.1.4. Fenton degradation of para-substituted phenols

The degradation of para-substituted phenols by the Fenton reagent (Fe^{2+}/H_2O_2) was carried out using different H_2O_2 concentrations (1.8 and 7.2 mM). In order to discriminate between the different substituents, slow degradation kinetics is desired. When the reaction starts, the solution becomes orange-brown within few minutes. Fig. 6 shows the *para*-substituted phenols degradation versus time for an initial H_2O_2 concentration of 1.8 mM. From this result, it was found that for the electron-donating substitutents (i.e. –H, –OCH_3 and –OH), the Fenton degradation process stops after 30 min treatment (with about 40, 50 and 30% degradation, respectively) even if H_2O_2 was not totally consumed. The p-OH, *p*-OCH_3, p-H and/or their degradation intermediates form stable complexes with iron. This complex formation induces an inhibition of initial compounds degradation since the iron ions were not available for a subsequent degradation. However, the degradation of intermediates continues and the production of polymers (tannins [10]) might

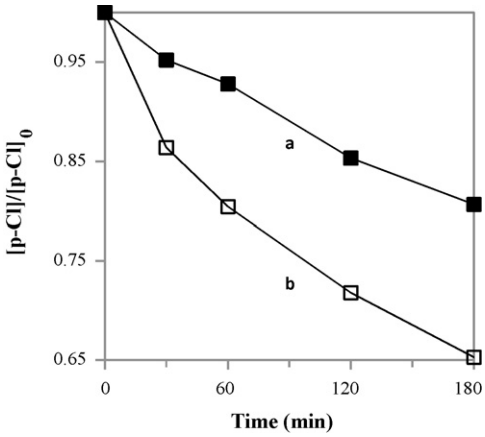

Fig. 5. Evolution of *p*-Cl concentration during degradation in the presence of Fe^{2+} (3 mg/L) at pH = 3 under: (a) dark conditions and (b) irradiation.

Table 1
Physico-chemical descriptors from literature and measured initial rate constants.

X	σ[a]	K_{ow}[b]	E_{HOMO}[c]	$E_{1/2}$[d]	E_{ZERO}[e]	λ_{max}[f]	pK_a[g]	r_0^{Fh}	r_0^{PFh}
NO_2	0.81	70.8	−10.07	1.17	4.28	316	7.65	0.046	0.070
Cl	0.28	309	−9.12	0.90	3.1	280	9.43	0.131	0.266
CHO	0.22	27.5	−9.49	n.d.	n.d.	284	7.62	0.073	0.201
H	0	30.2	−9.11	0.88	3.25	268	9.99	0.088	0.152
OCH_3	−0.28	37.2	−8.65	0.65	2.35	275	10.20	0.122	0.204
OH	−0.38	3.9	−8.72	0.42	2.36	288	9.91	0.127	0.195

[a] Hammett constants (σ) from [20].
[b] 1-Octanol/water partition coefficient (K_{ow}) from [30].
[c] Calculated energy of the highest occupied molecular orbital in eV from [30].
[d] Experimental half wave potential ($E_{1/2}$) from [31] in V.
[e] Calculated zero point corrected energies (E_{ZERO}) in eV from [32].
[f] Experimental maximal absorption wavelength (λ_{max}) in nm.
[g] Acidity constants (pK_a) from [30].
[h] Experimental initial degradation rate constants for Fenton (r_0^F) and photo-Fenton (r_0^{PF}) reactions in mM/min.

occur as well since no residual H_2O_2 was detected at the end of the treatment.

For the electron-withdrawing substituents, (i.e. –COH and $–NO_2$), the inhibition was not observed since the degradation continues until the H_2O_2 was totally consumed. The remaining H_2O_2 concentration was zero and 0.03 mM for *p*-CHO and *p*-NO_2, respectively. In the case of *p*-Cl, H_2O_2 final concentration was observed to be still high (>0.78 mM) despite the fast *p*-Cl degradation. Consequently these results suggest that *p*-Cl reacts via a different pathway than *para*-substituted phenols.

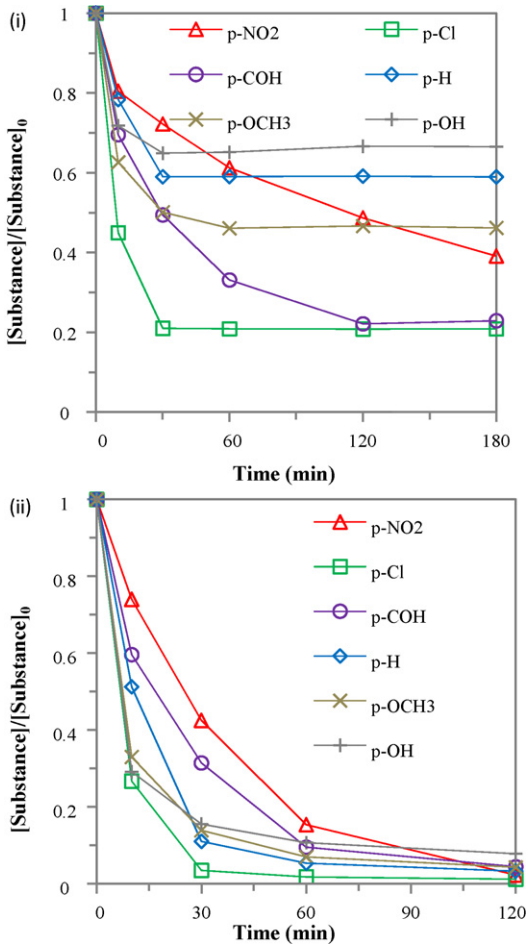

Fig. 6. Evolution of (i) *para*-substituted phenols concentration and (ii) TOC removal during Fenton degradation in the presence of Fe^{2+} (3 mg/L) at pH = 3 with H_2O_2 (i) 1.8 mM and (ii) 7.2 mM.

Fig. 6(ii) shows the *para*-substituted phenols degradation versus time for an initial H_2O_2 concentration of 7.2 mM. Under these conditions (closer to the optimal Fenton concentration), almost total degradation was achieved after 2 h for all the compounds and the reaction inhibition was not observed.

3.2. Photo-Fenton experiments

Fig. 7 depicts the evolution of the para-substituted phenol concentrations versus time for homogeneous photo-Fenton reaction with H_2O_2 7.2 mM. The results show that, except for *p*-NO_2, the degradation was fast reaching 80–90% in 15 min treatment. *p*-NO_2 was slowly degraded by TiO_2 [20] and is highly bio-recalcitrant [33]. The degradation of *p*-Cl was the fastest among the tested para-substituted phenols in analogy with Fenton oxidation (point 3.1.3). The compounds *p*-OCH_3, p-COH, p-OH have similar degradation rates confirming the low selectivity of photo-Fenton reaction. The substances degradation is faster as shown in Fig. 7 than in Fig. 6, confirming the light enhancement of the Fenton rates.

The TOC evolution during the treatment was followed next. From Fig. 8(i), for the 6-C compounds differences were observed in the initial degradation stages but the overall mineralization was similar, independently of the substituent nature. The differences between these compounds were in experimental error (2–3%). These observations confirm a low selectivity of photo-Fenton oxidation during mineralization. The fact that *p*-Cl degrades fast (point 3.1) did not distinguish *p*-Cl from the other para-substituted phenols in the mineralization process. For the compounds containing seven carbons, significant differences were observed between *p*-

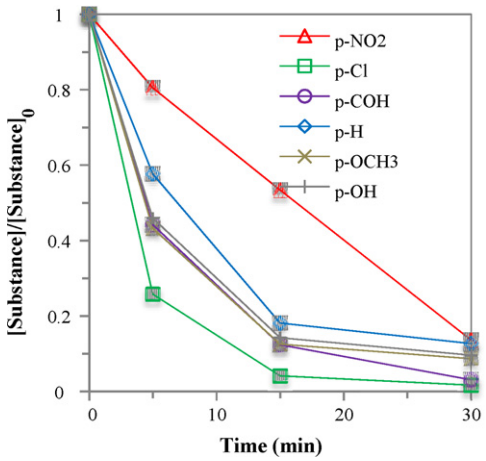

Fig. 7. Evolution of *para*-substituted phenols concentration, during photo-Fenton degradation in the presence of Fe^{2+} (3 mg/L) at pH = 3 with H_2O_2 7.2 mM.

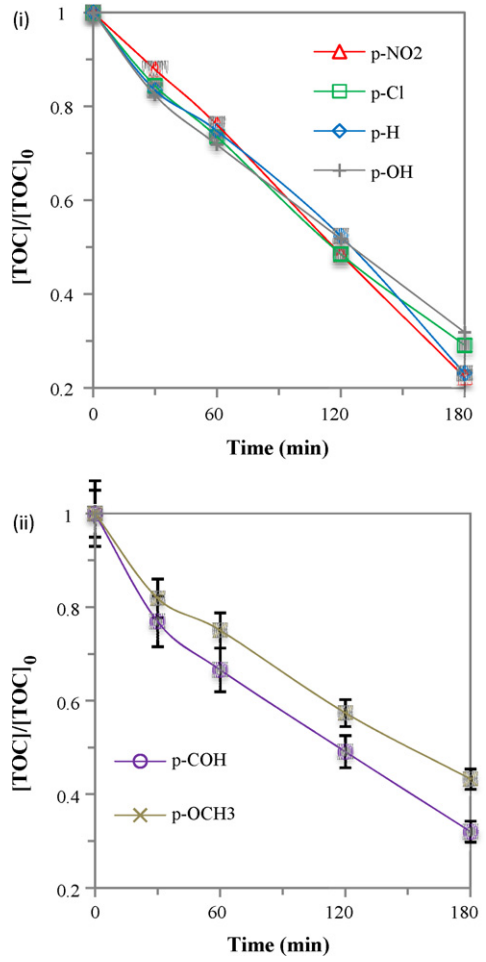

Fig. 8. TOC removal during *para*-substituted phenols photo-Fenton degradation in the presence of Fe^{2+} at pH = 3 with H_2O_2 15 mM for (i) six carbon constituted compounds and (ii) seven carbon constituted compounds.

CHO and *p*-OCH_3 (Fig. 8(ii)). The mineralization process was faster for *p*-CHO than for *p*-OCH_3 because the aliphatic carbon had an oxidation state of +I against zero for *p*-OCH_3. Eq. (10) suggests how the initial mineralization is accelerated in the case of *p*-CHO. After a first radical attack on the carbon positioned out of the ring, a complex formation may follow and a LMCT liberates a CO_2 molecule. For the *p*-OCH_3 more steps are needed to attain the same result:

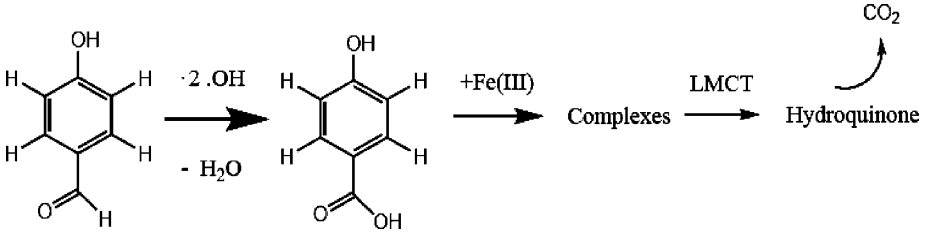

(10)

3.3. Quantitative structure reactivity relationship

3.3.1. QSRR for Fenton degradation

The relative initial rate of degradation (r_0^F) for *para*-substituted phenols and their corresponding descriptors are shown in Table 1. Linear regressions were performed plotting the initial Fenton rates (r_0^F) as a function of descriptors (results not shown). The correlation coefficients (R^2) are stated in Table 2. The *p*-Cl was excluded in this correlation due to its atypical reactivity (point 3.1). The plots of the electronic descriptors (E_{HOMO}, $E_{1/2}$, σ, E_{ZERO}) as a function of r_0^F show correlations with R^2 = 0.960, 0.976, 0.949, 0.994, respectively. E_{HOMO} and E_{ZERO} are calculated descriptors corresponding to the molecule electronic energy. The degradations were initially faster for molecules having low E_{HOMO} and E_{ZERO}. σ describes the effect induced by a given substituent on the electronic character of the aromatic ring. It was observed that the lower the Hammett constant, the fastest the degradation process due to the electrophilic nature of hydroxyl radical. $E_{1/2}$ describes the oxidation of phenols to phenoxyl radicals via Eq. (9). The fact that the degradation kinetics was related to $E_{1/2}$ suggests that electrophilic attack on the ring and on the alcohol group occur. The plots for log K_{ow}, pK_a, as a function of r_0 show a poor correlation.

The behavior of *p*-Cl is different from its analogues reacting faster than predicted by the model. This *p*-Cl deviation was reported by Parra et al. [20] for TiO_2 photocatalytic treatment and by Torres et al. [21] for electrochemical oxidation, possibly due to the low C–Cl dissociation energy (Table 3) and the high electronegativity of Cl.

Table 2
Correlation coefficients (R^2) obtained after linear regression in the plots of initial rates of degradation versus different descriptors.

	σ	K_{ow}	E_{HOMO}	$E_{1/2}$	E_{ZERO}	pK_a
Fenton degradation[a]	0.949	0.711	0.961	0.977	0.995	0.723
Photo-Fenton degradation[b]	0.975	0.679	0.996	0.847	0.986	0.662

[a] *p*-Cl excluded.
[b] *p*-Cl, *p*-CHO excluded.

Table 3
Homolytic dissociation energy of different bonds of the *para*-substituted phenols.

Compound	Weakest bond	Homolytic dissociation energy (kJ/mol)
p-Cl	C_6H_5-Cl	394
p-COH	C_6H_5CO-H	377
Other p-Xs	C_6H_5-H	460

3.3.2. QSRR for photo-Fenton degradation

The initial rate of photo-Fenton degradation (r_0^{PF}) for the different studied *para*-substituted phenols and their corresponding descriptors are represented in Table 1. These descriptors were used to establish a correlation with the initial degradation rates. Linear regressions were performed plotting initial Fenton rates (r_0^{PF}) as a function of descriptors (results not shown) and the correlation coefficients (R^2) are represented in Table 2. Although the plots of E_{HOMO}, $E_{1/2}$, σ, E_{ZERO} versus r_0 showed a poor correlation (results not shown), when *p*-Cl is evaluated separately and p-COH is not taken in account, a good correlation (R^2 = 0.996, 0.846, 0.975, 0.985, respectively) was observed. $E_{1/2}$ was a good descriptor in Fenton reaction but fails in the photo-Fenton system. Thus the reaction Eq. (9) probably plays a less significant role in photo-Fenton process. The other electronic parameters described well the reactivity when exclud-

Table 4
BOD_5 and ratio between (DBO_5) and (TOC) before and after photo-Fenton treatment.

Compound	BOD_5 (mg/L) before treatment	BOD_5/TOC	BOD_5 after photo-Fenton	BOD_5/TOC
p-OH	8	0.06	165	1.8
p-Cl	5	0.04	155	1.7
p-NO_2	5	0.04	145	1.6

ing *p*-CHO (that reacted in a "regular way" in Fenton treatment). K_{ow} and pK_a were found to poorly correlate with r_0^{PF}. The deviation observed for *p*-Cl is justified by previous observations (part 3.1.3, 3.1.4); for p-COH the presence of a weak bond (Table 3) and the proposed mechanism in Eq. (10) may explain this deviation.

3.4. Evolution of biodegradability of photo-Fenton treated solutions

To couple the photo-Fenton process with a biological treatment, it is important to know the biodegradability of the solutions after the Fenton treatment [33]. The amount of oxygen consumed in 5 days by aerobic microorganisms (BOD_5) was measured to determine if the substituent nature induced significant changes in the biodegradability of the treated solution. The experiments were performed using p-OH, *p*-Cl and *p*-NO_2 since these substances presents a variety of electronic properties, toxicity and photo-Fenton degradation rates. The photo-Fenton treatment was stopped when 30% TOC was mineralized.

The results presented Table 4 show that before treatment, the BOD_5 values were low (around 5 mg/L). Consequently, these solutions were poorly biodegradable. After the photo-Fenton treatment, an increase in the biodegradability was observed since the BOD_5 values were higher than 150 mg/L. No important differences were observed between these three substituents. The ratio between BOD_5 and TOC was calculated (Table 4). This parameter varies from around 0.05 before treatment to 1.8, 1.7 and 1.6 for p-OH, *p*-Cl and *p*-NO_2, respectively after treatment. For easily biodegradable water (like urban wastewater), with a ratio between BOD_5 and TOC being around 1.85, the results obtained show a substantial increase but poorly selective in the biodegradability due to photo-Fenton oxidation. A possible explanation for this observation is that the degradation intermediates are similar once the aromatic ring has been broken (aliphatic acids) implying a similar biodegradability for the intermediates in solution.

4. Conclusions

Para-substituted phenol reactivity is a function of the electronic effects induced by the substituents. The Fenton and photo-Fenton degradation is faster when the electronic density of the aromatic ring is high favoring electrophilic radical attack on the ring. The degradation rates are higher when half wave potential is low. These results suggest different reactions occurring at different positions on the molecule on the aromatic ring, alcohol function, or on the substituent. The electronic descriptors (experimental and calculated) fit well with the kinetic parameters particularly with the Fenton rates (excluding *p*-Cl) but also with the photo-Fenton degradation rates (excluding *p*-Cl and *p*-CHO). The photo-Fenton rates can be non-linearly correlated with electronic descriptors especially when the reaction occurs rapidly at the substituents for *p*-CHO or *p*-Cl. This is possibly due to the presence of weak bonds. The increase in biodegradability induced by photo-Fenton treatment was significant but poorly selective regarding specific substituents. This is probably due to the similarity of the degradation kinetics of the intermediates.

Acknowledgments

The authors wish to thanks the European Commission for its financial support under the INNOWATECH project (contract No 036882) within the thematic priority Global Change and Ecosystems of the Sixth Framework Program (FP6-2005-Global 4 - SUSTDEV-2005-3.II.3.2).

References

[1] N. Serpone, Relative photonic efficiencies and quantum yields in heterogeneous photocatalysis, J. Photochem. Photobiol. A: Chem. 104 (1997) 1–12.
[2] H. Chun, W. Yizhong, T. Hongxiao, Destruction of phenol aqueous solution by photocatalysis or direct photolysis, Chemosphere 41 (2000) 1205–1209.
[3] J. Arana, E. Tello Rendon, J.M. Dona Rodrıguez, J.A. Herrera Melian, O. Gonzalez Dıaz, J. Perez Pena, High concentrated phenol and 1,2-propylene glycol water solutions treatment by photocatalysis: catalyst recovery and re-use, Appl. Catal. B 30 (2001) 1–10.
[4] J. Villasenor, P. Reyes, G. Pecchi, Catalytic and photocatalytic ozonation of phenol on MnO_2 supported catalysts, Catal. Today 76 (2002) 121–131.
[5] G. Colon, M.C. Hidalgo, J.A. Navıo, Photocatalytic behaviour of sulphated TiO_2 for phenol degradation, Appl. Catal. B 45 (2003) 39–50.
[6] A. Sobczynski, L. Duczmal, W. Zmudzinski, Phenol destruction by photocatalysis on TiO_2: an attempt to solve the reaction mechanism, J. Mol. Catal. A: Chem. 213 (2004) 225–230.
[7] D. Vione, C. Minero, V. Maurino, M.E. Carlotti, M.E.T. Picatonott, E. Pelizzetti, Degradation of phenol and benzoic acid in the presence of a TiO_2-based heterogeneous photocatalyst, Appl. Catal. B 58 (2005) 79–88.
[8] G. Coloîn, J.M. Saĭnchez-Espanã, M.C. Hidalgo, J.A. Navîo, Effect of TiO_2 acidic pre-treatment on the photocatalytic properties for phenol degradation, J. Photochem. Photobiol. A: Chem. 179 (2006) 20–27.
[9] F. Herrera, C. Pulgarin, V. Nadtochenko, J. Kiwi, Accelerated photo-oxidation of concentrated p-coumaric acid in homogeneous solution. Mechanistic studies, intermediates and precursors formed in the dark, Appl. Catal. B 17 (1998) 141–156.
[10] J. Arañã, E. Tello-Rendoîn, J.M. Doñã-Rodrîguez, C. Valdeĭs Do Campo, Highly concentrated phenolic wastewater treatment by heterogeneous and homogeneous photocatalysis: mechanism study by FTIR-ATR, Water Sci. Technol. 44 (2001) 229–236.
[11] A. Goi, M. Trapido, Hydrogen peroxide photolysis, Fenton reagent and photo-Fenton for the degradation of nitrophenols: a comparative study, Chemosphere 46 (2002) 913–922.
[12] W. Gernjak, T. Krutzler, A. Glaser, S. Malato, J. Caceres, R. Bauer, A.R. Fernaĭndez-Alba, Photo-fenton treatment of water containing natural phenolic pollutants, Chemosphere 50 (2003) 71–78.
[13] V. Kavitha, K. Palanivelu, The role of ferrous ion in Fenton and photo-Fenton processes for the degradation of phenol, Chemosphere 55 (2004) 1235–1243.
[14] H. Kusicĭ, N. Koprivanac, A.L. Bozicĭ, I. Selanec, Photo-assisted Fenton type processes for the degradation of phenol: a kinetic study, J. Hazard. Mater. 136 (2006) 632–644.
[15] J.M. Tseng, C.P. Huang, Removal of chlorophenols from water by photocatalytic oxidation, Water Sci. Technol. 23 (1991) 377–387.
[16] J.–C. D'Oliveira, C. Guillard, C. Maillard, P. Pichat, Photocatalytic destruction of hazardous chlorine- or nitrogen-containing aromatics in water, J. Environ. Sci. Heal. A: Environ. Sci. Eng. 28 (1993) 941–962.
[17] K.E. O'Shea, C. Cardona, Hammett study on the TiO_2-catalyzed photooxidation of para-substituted phenols. A kinetic and mechanistic analysis, J. Org. Chem. 59 (1994) 5005–5009.
[18] L. Amalric, C. Guillard, E. Blanc-Brude, P. Pichat, Correlation between the photocatalytic degradability over TiO_2 in water of meta and para substituted methoxybenzenes and their electron density, hydrophobicity and polarizability properties, Water Res. 30 (1996) 1137–1142.
[19] A. Assabane, Y. Ait Ichou, H. Tahiri, C. Guillard, J. -M. Herrmann, Photocatalytic degradation of polycarboxylic benzoic acids in UV-irradiated aqueous suspensions of titania. Identification of intermediates and reaction pathway of the photomineralization of trimellitic acid (1,2,4-benzene tricarboxylic acid), Appl. Catal. B 24 (2000) 71–87.
[20] S. Parra, J. Olivero, L. Pacheco, C. Pulgarin, Structural properties and photoreactivity relationships of substituted phenols in TiO_2 suspensions, Appl. Catal. B 43 (2003) 293–301.
[21] R.A. Torres, W. Torres, P. Peringer, C. Pulgarin, Electrochemical degradation of p-substituted phenols of industrial interest on Pt electrodes. Attempt of a structure–reactivity relationship assessment, Chemosphere 50 (2002) 97–104.
[22] M. Lapertot, P. Pichat, S. Parra, C. Guillard, C. Pulgarin, Photocatalytic degradation of p-halophenols in TiO_2 aqueous suspensions: halogen effect on removal rate, aromatic intermediates and toxicity variations, J. Environ. Sci. Heal. A: Environ. Sci. Eng. 41 (2006) 1009–1025.
[23] G. Palmisano, M. Addamo, V. Augugliaro, T. Caronna, A. Di Paola, E. García López, V. Loddo, G. Marci, L. Palmisano, M. Schiavello, Selectivity of hydroxyl radical in the partial oxidation of aromatic compounds in heterogeneous photocatalysis, Catal. Today 122 (2007) 118–127.

[24] C. Karunakaran, R. Dhanalakshmi, Substituent effect on nano TiO_2- and ZnO-catalyzed phenol photodegradation rates, Int. J. Chem. Kinet. 41 (2006) 275–283.
[25] L. Byung-Dae, I. Mamoru, H. Masaaki, Prediction of Fenton oxidation positions in polycyclic aromatic hydrocarbons by Frontier electron density prediction of Fenton oxidation positions in polycyclic aromatic hydrocarbons by Frontier electron density, Chemosphere 42 (2001) 431–435.
[26] V. Kavitha, K. Palanivelu, Degradation of nitrophenols by Fenton and photo-Fenton processes, J. Photochem. Photobiol. A: Chem. 170 (2005) 83–95.
[27] J. Kiwi, C. Pulgarin, P. Peringer, Effect of Fenton and photo-Fenton reactions on the degradation and biodegradability of 2 and 4-nitrophenols in water treatment, Appl. Catal. B 3 (1994) 335–350.
[28] G. Ruppert, R. Bauer, G. Heisler, S. Novalic, Mineralization of cyclic organic water contaminants by the Photo-Fenton reaction influence of structure and substituents, Chemosphere 27 (1993) 1339–1347.
[29] X. Sun, T. Sun, Q. Zhang, Degradation mechanism of PCDDs initiated by OH radical in Photo-Fenton oxidation technology: quantum chemistry and quantitative structure–activity relationship, Sci. Total Environ. 402 (2008) 123–129.
[30] A.O. Aptula, T.I. Netzeva, I.V. Valkova, M.T.D. Cronin, T.W. Schultz, R. Khune, G. Schurmann, Multivariate discrimination between modes of toxic action of phenols, Quant. Struct. -Act. Relat. 21 (2002) 12–22.
[31] M.J.B. Hauser, L.F. Olsen, The role of naturally occurring phenols in inducing oscillations in the peroxidase–oxidase reaction, Biochemistry 37 (1998) 2458–2469.
[32] K.C. Gross, P.G. Seybold, Substituent effects on the physical properties and pK_a of phenol, Int. J. Quantum Chem. 85 (2001) 569–579.
[33] J. Bandara, C. Pulgarin, P. Peringer, Chemical (photo-activated) coupled biological homogeneous degradation of p-nitro-o-toluene-sulfonic acid in a flow reactor, J. Photochem. Photobiol. A 111 (1997) 253–263.